QUASAR EVOLUTION DERIVED FROM THE PALOMAR BRIGHT QUASAR SURVEY AND OTHER COMPLETE QUASAR SURVEYS

MAARTEN SCHMIDT

Palomar Observatory, California Institute of Technology

AND

RICHARD F. GREEN

Steward Observatory, University of Arizona Received 1982 August 11; accepted 1982 December 3

ABSTRACT

We present the Bright Quasar Survey (BQS) consisting of 114 objects to an average limiting magnitude B=16.16 over an area of 10,714 deg². There are 92 quasars with $M_B<-23$ in the sample. We use the BQS and complete samples from published surveys to derive models of the statistical evolution of quasars. The increase of space density with redshift depends strongly on absolute luminosity, being close to zero for low-luminosity quasars. Detailed predictions are given for the distribution of redshifts and magnitudes and for the total counts based on the evolution models. Subject headings: cosmology—luminosity functions—quasars

I. INTRODUCTION

We present in this paper a derivation of the optical luminosity function of quasars and its evolution, based on a new survey of bright optically selected quasars and other published quasar surveys.

Early work on the quasar luminosity function was based on quasi-stellar radio sources in the 3CR, 4C, Parkes, and NRAO catalogs. Samples complete to given limits in these catalogs showed evidence for evolution, in the sense that the comoving space density of quasars increases with redshift (Schmidt 1968, 1974b; Lynds and Wills 1972; Wills 1974). Subsequently, it appeared that quasars with flat radio spectra exhibit less evolution (Schmidt 1976, 1978; Masson and Wall 1977; Wills and Lynds 1978), but evolution similar to that of steep-spectrum quasars was found by Blake (1978) and Peacock et al. (1981). Recent studies of samples of extragalactic radio sources, made up of radio galaxies and quasars, show an evolution increasing with radio luminosity, but the dependence on radio spectral index is still uncertain (Wall, Pearson, and Longair 1980, 1981; Peacock and Gull 1981).

Most quasars selected on the basis of purely optical criteria do not appear in the major radio catalogs mentioned above. We may consider the optically selected quasars as the parent population from which the quasistellar radio sources are drawn. The Braccesi survey (Braccesi, Formiggini, and Gandolfi 1970) yielded the only published list of optically selected quasars for almost a decade. Available spectroscopic coverage of the blue stellar objects in the survey allowed construction of

a modest sample complete to eighteenth magnitude. The magnitude distribution of these quasars suggested evolution similar to that of steep-spectrum radio quasars (Schmidt 1978). The concept of luminosity evolution of quasars was explored by Mathez (1978), Braccesi et al. (1980), and Cheney and Rowan-Robinson (1981a). The statistical basis for studies of the evolution of optically selected quasars has improved over the past five years with the publication of several objective-prism and grating-prism surveys. These surveys have yielded large numbers of quasars, mostly of high redshift.

In this paper we present the Bright Quasar Survey (BQS) which contains 114 objects to an average limiting magnitude $B_{\rm lim} = 16.16$, of which 92 are quasars with $M_B < -23$. We use all the surveys of optically selected quasars together to address the question of the statistical evolution of quasars.

The organization of this paper is as follows. The next section covers the relation between flux densities, B magnitudes, and AB magnitudes for an assumed shape of the spectral energy distribution of quasars. In § III we discuss the construction of the Bright Quasar Survey from the PG survey of blue stellar objects. The derivation of complete samples from other published surveys is addressed in § IV. In § V we discuss counts of bright quasars and their relation to the distance scale. The procedure for the derivation of the statistical evolution of quasars is presented in § VII. The distributions of redshifts and magnitudes, and the counts, predicted by the evolution models, are given in § VIII. The number of quasars with z > 3.5 expected on the basis of the models

is discussed in § IX. In three brief appendices we discuss some alternative evolution models, objects of low luminosity, and pure luminosity evolution.

II. PHOTOMETRIC SYSTEMS FOR QUASARS

Photometry plays an important role in the derivation of the evolution from quasar samples for two reasons. First, the limiting apparent magnitude of the quasar sample is required to derive the volume accessible to each quasar, which is needed to derive the luminosity function. The limiting magnitude is by necessity in the observer's frame of reference. Second, the apparent magnitude of a given quasar in conjunction with its redshift determines its absolute magnitude. This absolute magnitude should refer to a given rest wavelength, in the frame of the quasar.

With quasar redshifts ranging from 0.1 to 3.5, the apparent flux at a given rest wavelength is in general not available. In practice, we use an average spectral energy distribution which allows us to derive the flux at the required wavelength from the observed flux. On the basis of the energy distributions given by Richstone and Schmidt (1980) we adopt a power-law spectrum, $f_{\nu} \sim \nu^{\alpha}$, with spectral index $\alpha = -0.5$. This power-law spectrum applies redward of Ly α at 1216 Å only: at shorter wavelengths the typical quasar shows a systematic deficiency (Green *et al.* 1980; Oke and Korycansky 1982).

The adopted power-law spectrum is only an approximation. The spectral index α shows a considerable spread, and the mean continuum exhibits systematic departures from a perfect power law (Richstone and Schmidt 1980). In addition, there are emission lines and sometimes absorption lines. All these effects generate deviations from the $\alpha = -0.5$ power-law spectrum that we loosely estimate to be no less than 0.2 mag on the average. Compared to these uncertainties, the effect of galactic absorption is relatively small: above latitude 30°, where most of the quasars in the sample are located, the range of absorption is not much more than 0.1 mag. Accordingly, we have made no corrections for galactic absorption. When measurements of the individual energy distributions and line strengths of BQS quasars are completed and reduced, it will be worthwhile also to account for galactic absorption.

Since the Bright Quasar Survey is based on B magnitudes, we have used these throughout most of this paper. Observers of high-redshift quasars use different magnitudes (for details, see § IV) related to the AB system. Oke (1974) defined the magnitude system AB in terms of flux density $f_{\nu}(\lambda)$ in units of ergs s⁻¹ cm⁻² Hz⁻¹ as

$$AB = -2.5 \log f_{\nu}(\lambda) - 48.60. \tag{1}$$

By definition, AB = V for $\lambda = 5500$ Å. The *B* magnitude has an effective wavelength around 4400 Å. Oke and Schild (1970) and Hayes and Latham (1975) find that

 α Lyrae is 0.24 mag brighter in f_{ν} at 4400 Å than at 5500 Å. Since α Lyrae has B - V = 0, this calibration leads to

$$B = -2.5 \log f_{\nu}(4400) - 48.36. \tag{2}$$

For a power-law energy distribution with spectral index $\alpha = -0.5$, the relation between B and flux density $f_{\nu}(\lambda)$ is

$$B = -2.5 \log f_n(\lambda) + 1.25 \log (\lambda/4400) - 48.36.$$
 (3)

The systematic deviation from the power-law spectrum below 1216 Å, together with Ly α emission, affects B by less than 0.2 mag for z < 3.1, i.e., no more than typical deviations at longer wavelengths due to lines, etc., discussed above.

For redshifts larger than 3.1 we cannot use B any more, and we will use the AB magnitude at 6500 Å, well beyond Ly α for all quasars with known redshifts. For redshifts sufficiently low that both the B filter and AB(6500) measure the $\alpha = -0.5$ power-law spectrum of a quasar, their relation is simply

$$B - AB(6500) = 0.45. (4)$$

III. THE PALOMAR BRIGHT QUASAR SURVEY

In this section we discuss the selection of objects for inclusion in the Palomar Bright Quasar Survey, as well as the problem of confusion with Seyfert I galaxies.

a) Selection of the Sample

The Palomar Bright Quasar Survey (BQS) is a subset of the larger Palomar-Green Survey (PG) of stellar objects with ultraviolet excess. The area surveyed is 10,714 deg² in absolute galactic latitudes above 30°, covered by 266 double U and B exposures from the Palomar 18 inch (46 cm) Schmidt telescope. The films were processed with the PDS scanning microdensitometer and computing facilities of the Image Processing Laboratory of the Jet Propulsion Laboratory (Green and Morrill 1978) to produce a catalog of photographic magnitudes and colors. After standardization with photoelectrically measured comparison stars, objects were selected on the basis of the color criterion U-B <-0.44. All 1800 objects in the PG catalog have been observed by slit spectroscopy. Spectroscopic classifications were obtained for all but about 10 objects with poorly observed spectra: these are all suspected to be stars. The redshift for each quasar found depends on at least two emission lines. A full description of the observational techniques will be given in a paper presenting the PG catalog (Green, Schmidt, and Liebert 1983).

The U-B colors derived from the photographic 18 inch Schmidt exposures have an rms error of ± 0.24 mag. As a consequence of the U-B=-0.44 cutoff and

the errors in the U-B colors, some quasars will be missed in the PG catalog. If the U-B colors in the quasar catalog of Hewitt and Burbidge (1980) are representative, then we estimate that around 12% of quasars have escaped inclusion in the PG catalog. We expect to provide more reliable information about the completeness of the PG catalog on the basis of a study of parts of fields covered by more than one photographic exposure.

The photographic B magnitudes have an rms error of ± 0.27 mag. The quasar counts will be systematically affected by the errors in B. Assuming that the error distribution is Gaussian with dispersion σ , the correction to the observed counts is $-(\sigma^2/2)(d^2n/dB^2)$, where n = n(B) represents the differential counts (see Eddington 1940). For a logarithmic slope of the differential counts, which (on the basis of the cumulative counts discussed in § V) we estimate to be $d(\log n)/dB = 0.90$, and $\sigma = \pm 0.27$ mag, the correction to the counts is -15%. We have not made any corrections for the effects of incompleteness and overestimation, which at present appear to be of the same order.

The limiting magnitude $B_{\rm lim}$ of each of the 266 fields was determined from the instrumental measures. The coverage of the PG catalog is defined by 74 different values of $B_{\rm lim}$ together with the associated areas of the sky in square degrees (see Table 1 in Green, Schmidt, and Liebert 1983). The limiting magnitudes range from 15.46 to 16.63 for an effective limiting magnitude $B_{\rm lim} = 16.16$.

The BQS consists of all objects in the PG catalog that fulfill certain morphological and spectroscopic criteria. The morphological criterion is that the object should have a dominant starlike appearance on blue prints of the 48 inch (1.2 m) Schmidt Sky Atlas. In practice, this means that most of the light should originate from within an angular diameter of $\sim 2''$. The judgment as to whether the starlike component of the light is "dominant" depends on the telescope used. Our definition is based on the Sky Atlas prints as the best compromise between uniformity and availability.

The spectroscopic criterion for inclusion in the Bright Quasar Survey is that the object should show broad emission lines with substantial redshift. The smallest redshift listed in our survey is 0.025; hence there is no confusion with objects belonging to our Galaxy for which the redshift is at most 0.002. The line width criterion is essentially the same as that used to classify Seyfert I galaxies. Hence, we have not included in the Bright Quasar Survey 22 extragalactic objects in the PG

survey that have narrow emission lines, such as those observed in Seyfert II galaxies. Their absolute luminosities, M_B , are relatively low, between -22 for Mrk 684, which is the nucleus of a spiral galaxy, and -15 for Mrk 36. Not included in the BQS are three BL Lac objects in the PG catalog, which showed continuous spectra from 3000 to 9500 Å.

The total number of objects selected for inclusion in the BQS on the basis of the above criteria is 114. Information about each of these objects is presented in Table 1, including a position usually accurate to 1", redshift, photographic B magnitude, the limiting magnitude $B_{\rm lim}$ in its discovery field, one cross reference² if previously known, absolute magnitudes M_B , and model-dependent quantities to be discussed in § VII. Finding charts for those objects without charts in the literature are found in Figure 1 (Plates 6 and 7). Table 2 presents the cumulative surface density of these objects as a function of B magnitude.

b) Confusion with Seyfert I Nuclei

The range of absolute magnitudes M_B of objects in the Bright Quasar Survey is from -20.7 to around -30. There is considerable overlap with luminosities of Seyfert I nuclei, the brightest of which has $M_B \approx -23$. As a matter of fact, some of the low-luminosity objects in the BQS have been classified as Seyfert I galaxies on the basis of morphological classification with larger telescopes. Examples are II Zw 136, III Zw 2, and many of the objects with Markarian designations.

For all BQS objects less luminous than $M_B = -24.1$, we have indicated in Table 1 whether on the prints of the Palomar Sky Atlas the object has a stellar appearance or shows associated nebulosity. We are unable to decide which of these objects are low-luminosity quasars with associated nebulosity and which are Seyfert I nuclei. In fact, the distinction may make no fundamental sense in that the Seyfert I nuclei may be small-scale quasars.

Some objects of higher absolute luminosities also show associated nebulosity. For example, Wyckoff, Wehinger, and Gehren (1981) have resolved 13 quasars, including 3C 273 with $M_B = -27$. Boroson, Oke, and Green (1982) showed from off-nuclear spectra that five of the BQS quasars with $M_B < -23$ are embedded in nebulosity dominated by starlight.

For the purposes of this paper, we will make a distinction based on absolute luminosity. We will refer to the 92 objects brighter than $M_B = -23$ as quasars and to the 22 objects of lower luminosity as Seyfert I nuclei or low-luminosity quasars. A discussion of these lower luminosity objects is found in Appendix B.

¹Quasars in the redshift range 0.6-0.8 appear to be the reddest in U-B (for redshifts less than 2.15), probably due to the combined effect of Mg II emission and the 3000 Å bump in the B filter. We estimate the PG catalog to be 72% complete in this redshift range. The relative scarcity of quasars with such redshifts in the BOS (see Fig. 3) may be partly due to this effect.

²PB refers to the Palomar-Berger blue star survey (Berger and Fringant 1977) and K to the Kiso blue star survey (Noguchi, Machara, and Kondo 1980).

TABLE 1
THE PALOMAR BRIGHT QUASAR SURVEY

109(1/V2)	(HL5)	-3.25	+1.04	-1.17	-4.49	+1.12	40.08	10.80	+1.07	-1.24	-0.19	40.29	900	+1.72	10.0	+1.56	-7.41	-0-49	-2.52	-0.24	-1.35	-3.52	4.00	+1,70	-0.62	-2.28	74.47	-2.95	0.10	-9.39	-0.25	-1.47	1 0 0	+0.90	-9.33	-6.75	+1.21	1.00	-1.4/	-0.35	-2.66	-10.34	-4.77	+0.21	-9.02	+1.63	-10.29	-6.51
1 og ((HH2)	-3.27	+0.42	-1.33	-4.37	+0.98	60.0	7.03	40.04	-1.40	-0.36	+0°.12	20.0	+1.68	1 1	+1 42	-6.85	-0.66	-2.60	-0.41	-1.51	-3.52	0 0 0 0	+1-65	-0.79	-2.38	2.7.	-2.99	-0.27	-8.47	-0.43	-1.62	10.1	+0.76	-8.42	-6.30	+1.09	-1.22	-1.02	-0.52	-2.74	-9.17	-4.61	+0.0+	-8.17	+1.58	-9.13	-6.10
Æ	(d=0°5)	-26.19	-22.53	-24.70	-25.92	-22.04	-23.43	-24.42	-22.10	-24.76	-23.74	-23.17	-23.42	-20.99	124.24	-21.09	-28.27	-24.04	-25,73	-23.79	-24.86	-26.35	-22.22	20.10-	-24.19	-25.57	-25.70	-26.00	-23.63	-29.16	-23.81	-24.96	-24.71	-22,35	-29.13	-27.97	-21.88	-24.61	-28.40	-23.91	-25.82	-29.87	-27.02	-23.27	-28.99	-21.15	-29.82	-27.86
log(1/V2)	(HL1)	-2.98	+1.06	98.0	-4.32	+1.10	+0.29	0.01	+1.07	-0.94	+0.03	40.45	0 :	+1.71		+1.55	-7.91	-0.27	-2.15	-0.03	-1.07	-3,32	+1.00 5.00	+1.49	-0.38	-1.99	2.7. 1.7.	-2.67	40.11	-10.59	40.0	-1.15	10.0	+0.93	-10.62	-6.98	+1.20	B !	. מ ניים	0,10	-2.34	-11.98	-4.23	+0.41	-9.78	+1.62	-11.91	-6.77
1 og ((HH1)	-3.13	+1.04	-1.09	-2. /1 -4. 38	+1.09	40.04	10.0	30.	-1.16	-0.17	+0.27	-0.32	+1.71	0.01	11.55	-7.52	40	-2,35	-0.24	-1.30	-3.45	+0.97	+1 40	09.0	-2.20	12.5	-2.84	-0.10	-9.79	0.25	-1.38	10.03	88 0+	-9.81	-6.71	+1.20	-1.00	2.5/	-0.31	-2.53	-10.89	-4.29	+0.22	-9.11	+1.62	-10.84	-6.53
£	(q=0.1)	-26.38	-22.14	-24.76	-25.09	-22.07	-23.45	-24.44	-22,12	-24.83	-23.78	-23.23	-23.95	-21.00	-24.52	-21.12	-28.75	-24.15	-25.83	-23.86	-24.96	-26.58	-22.24	-21.05	-24.26	-25.71	-25.85	-26.18	-23.69	-29.79	-23.87	-25.03	-24.71	-22,38	-29.80	-28.36	-21.90	-24.68	-25.05	-23,94	-25.97	-30.59	-27.09	-23.30	-29.48	-21.17	-30.54	-28.27
	REMARKS	PHL 658	MK 335		PB 6151 PKS	MK 1148	I Zw 1			MK 1014			104 NO.	TK 110	100 NO.	2		K 347-45	K 348-7		4C 13.41			MK 142	1	3C 246	TF 249 1	PKS	!	TRIPLE		TON 1388	#C/ YE	MK 1298		LB 2126		1	ea com			TON 1530	3C 273	TON 1542			LB 19	
	NEB ?		* c	1		*	neb				*	neb	ge.	neb	4					*			×	q					*		neb	1	ga.	*			neb			*				neb		*		
	Z																																															
	B _{lim} N	16.08	16.16	16.14	16.14	16.02	16.02	16.23	10.00	15.97	16.45	16.45	15.71	16.35	10.41	10.27	16.19	16.41	16.28	16.16	16.35	16.35	16.33	16.55	15.84	16.02	16.21	16.21	16.23	16.09	16.20	15.86	16.12	16.28	16.29	16.39	16.15	15.84	15.80	15.79	15.81	15.61	16.11	15.61	15.79	16.24	15.99	16.21
	€			14.95 16.14				- '		. –	_	_	-	15.62 16.35	٠.	-	• -	-	15.05 16.28	-	-	-	15.49 16.33	-	-	16.00 16.02	. 10.	16.	•	_	16.02 16.20	. ,	-	-		_		,	15.02 15.80		-	_		_		_	_	_
	Blim	15.96	13.75		15.88	15.88	14.39	15.42	10.03	15.20	15.15	16.30	14.00	15.62	10.04	14.73	16.00	16.40	15.05	16.13 1	15.93 1	16.24	15.49	10.07	15.81	16.00 16.	15.75 16.	16.07 16.	16.05	15.84	16.02	15.17	14.00	15.43	16.05	15.82	15.46	15.51	15.02	14.63	15.68	15.49	12.86	14.65	15.38	16.15	15.53	16.06
	B B _{lim}	07 0.450 15.96	55 30 0.025 13.75	14.95	54 41 0.384 15.88 03 35 0.624 15.97	09 41 0.064 15.88	25 19 0.061 14.39	24 0.155 15.42	54 45 0 054 15.03	09 10 0.164 15.20	11 32 0.100 15.15 1	03 59 0.131 16.30	56 09 0.064 14.00 1	30 14 0.035 15.62 1	0.190 16.04 1	19 11 0 050 14.73 1	09 19 1,216 14,00 1	40 54 0 204 16 40 1	29 39 0.239 15.05 1	27 35 0.161 16.13 1	03 38 0.240 15.93 1	19 02 0.553 16.24 1	77 0 105 15.49 1	55 40 0 045 14.19 1	15 23 0.167 15.81 1	02 13 0.344 16.00 16.	0.35/ 15.75 16.	36.38 0.425 16.02 16.	30 01 0.144 16.05 1	02 24 1.722 15.84 1	14 0.154 16.02 1	35 43 0.177 15.17 1	54 0 234 14.63	07.35 0.060 15.43	03 38 1.876 16.05 1	54 13 0.969 15.82 1	05 34 0.049 15.46 1	45 10 0.176 15.51	0.169 15.02	19 53 0.085 14.63 1	55 19 0.334 15.68 1	51 49 2.046 15.49 1	19 42 0.158 12.86 1	03 0.064 14.65 1	37 29 1.273 15.38 1	38 31 0.048 16.15 1	47 28 2.038 15.53	07 58 1.030 16.06 1
	950) z B B _{lim}	03 25.0 +15 53 07 0.450 15.96	+19 55 30 0.025 13.75	26 38.1 +12 59 30 0.142 14.95	+03 54 41 0.384 15.88 +03 03 35 0.624 15.97	49 16.5 +17 09 41 0.064 15.88	50 57.8 +12 25 19 0.061 14.39	52 11.1 +25 09 24 0.155 15.42	57 0 +27 54 35 0 053 15.03 1	57 16.3 +00 09 10 0.164 15.20 1	04 35.4 +76 11 32 0.100 15.15 1	38 32.0 +77 03 59 0.131 16.30 1	+34 56 09 0.064 14.00 1	21 44.4 +52 30 14 0.035 15.62 1	25 05.8 +20 0/ 0/ 0.190 16.04 1	23 20.2 +12 3/ 08 0.027 14.73 1 34 34 5 +01 19 11 0 050 14 39 1	46.7 +30.09.19 1.216 14.00 1	47 44 B +39 40 54 0 204 14 40 1	53 48.3 +41 29 39 0.239 15.05 1	01 43,3 +05 27 35 0.161 16.13 1	04 45.1 +13 03 38 0.240 15.93 1	08 30.0 +13 19 02 0.553 16.24 1	03 43 0.058 15.49 1	22 22 40 48 33 0.183 13.87 1	48 56.1 +34 15 23 0.167 15.81 1	48 59.4 -09 02 13 0.344 16.00 16.	35 20 0.35/ 15.75 16.	03 58.1 -00 34 38 0.425 14.02 16.	14 20.5 +44 30 01 0.144 16.05 1	15 41.5 +08 02 24 1.722 15.84 1	15 46.2 +40 42 14 0.154 16.02 1	1 16 30.1 +21 35 43 0.177 15.17 1	14 54 0 034 14.63	43.6 -04.07.35 0.060 15.43 1	38 42,4 +04 03 38 1,876 16,05 1	48 42.6 +54 54 13 0.969 15.82 1	49 30.9 -11 05 34 0.049 15.46 1	51 15.7 +11 45 10 0.176 15.51 1	02 08.9 +28 10 54 0.165 15.02 1	11 44.8 +14 19 53 0.085 14.63 1	47.2 +06 55 19 0.334 15.68 1	22 56.6 +22 51 49 2.046 15.49 1	26 33.4 +02 19 42 0.158 12.86 1	29 33.1 +20 26 03 0.064 14.65 1	41.0 +17 37 29 1.273 15.38 1	44 02.1 +02 38 31 0.048 16.15 1	39.0 +26 47 28 2.038 15.53 1	48 26.6 +40 07 58 1.030 16.06 1

TABLE 1—Continued

								1		100	1	722.	
					1			e E	1001	10g(1/Va)	8 E	10g(1/Va)	e e
PG	R.A. (1950)	DEC. (1950)	Z	20	Blim	NEB ?	REMARKS	(q=0.1)	(HH1)	(HL1)	(d=0:5)	(HH2)	(HL5)
1302-102	8		0.286	15.09	16.04		PKS	-26.20	-2.87	-2.69	-26.08	-3.10	-3.07
1307+085	0		0.155	15.28	16.30			-24.63	-0.95	-0.72	-24.56	-1.18	-1.01
1309+355		31	0.184	15.45	15.96		TON 1565	-24.84	-1.17	-0.94	-24.76	-1.40	-1.24
1310-108	2		0.035	15.55	16.04	*		-21.07	+1.67	+1.67	-21.06	+1.64	+ 08
1322+659	7 7	2	0.168	15.86	16.08			-29.63	-9.43	-10,16	-28.94	9.0	92
13274412	44 44	40	1.730	15.44	10.00		PB 4007	-27.19	-4.46	-4.42	-26.95	-4.50	-4.63
1338+416	9 89	+41 38 18	1.219	16.08	16.30		1	-28.67	-7.37	-7.73	-28.20	-6.72	-7.25
1341+258	41 36.	53	0.087	15.93	16.17	neb	TDN 730	-22.69	+0.66	+0.75	-22.66	+0.53	+0.68
1351+236	51 46.	40	0.055	15.87	16.17	*	MK 662	-21.74	+1.29	+1.29	-21.72	+1.20	+1.30
1351+640	51 46.	8	0.087	15.42	16.10	*		-23.20	+0.29	+0.47	-23.17	÷ 13	+0.29
52+18	52 12.	20	0.158	15.71	15.86		PB 4142	-24.24	9.28	-0.36	-24.17	-0.77	9.6
1352+011	13 52 25.8	9 ;	0.435	16.03	16.06			-26.23	-2.41	-2.74	-26.04		250
14004+215		67 BI 17+	0.500	15.57	16.08		TON 187	-24.46	-0-79	-0.56	-24.39	-1.00	-0.83
1404+226	04 02	37	0.098	15.82	16.08	*	701	-23.07	+0.39	+0.54	-23.02	+0.24	+0.41
1407+265	07 07.	+26 32 30	0.944	15.73	15.99	·		-28.39	-6.77	-7.04	-28.00	-6.36	-6.82
1411+442	11	14	0.089	14.99	16.09	*	PB 1732	-23.68	-0.09	+0.11	-23.65	-0.28	-0.11
1415+451	14 15 04.3	60	0.114	15.74	16.09	*		-23.48	+0.07	+0.27	-23.43	0.0	+0.07
1416-129	16 21.	8 :	0.129	15.40	15.86	*	0	724.10	,	0.23	124.04	0.0	• 0 • 0
1425+267	n à	+26 45 38	0.366	15.67	16.00	•	100 ZOZ	-23,55	40.0	+0.22	-23.51	3 4	+0
1427+480	14 20 55.0	9 8	223	15.55	16.34	•	201	-24.37	-0,70	-0.48	-24.28	-0.88	-0.71
1435-067	35 37	5	0.129	15.54	15.74	*		-23.96	-0.32	-0.11	-23.90	-0.51	-0.34
1440+356	40 04.			15.00	16.04	*	MK 478	-23.35	+0.17	+0.36	-23.32	0°0	+0.17
1444+407	44	47		15.95	16.14			-25.18	-1.55	-1.32	-25.07	-1.75	-1.61
1448+273	48 58	21	0.065	15.01	15.86	neb		-22.47	+0.46	+0.09	-22.94	÷.	+0.47
1501+106	01 36.	3	0.036	15.09	16.21	*	MK 841	-25.00	12.57	12.27	BC:17-	+1.27	11.00
1519+226	15 19 02 1		0.137	15.09	16.12	*		-23,54	+0.02	+0.22	-23.48	-0.14	+0.03
1522+101	23	8		15.74	15.88			-29.22	-8.53	-9.09	-28.71	-7.66	-8.39
1534+580	34		0.030	15.54	16.33	neb	MK 290	-20.75	+1.86	+1.86	-20.73	+1.85	+1.87
1535+547	35 21.	54	0.038	15.31	16.40	neb	I Zw 120	-21.49	+1.43	+1.43	-21.48	+1.36	+1.44
1568+4//		ֆ լ Ն լ	0//0	16.01	16.14			-26.01	-2.60	-2.41	-25.84	-2.76	-2.69
1545+210	45 31.		0.266	16.05	16.09		30 323.1	-25.08	-1.42	-1.20	-24.96	-1.62	-1.48
1552+085	52	31	0.119	16.02	16.04	*		-23.30	+0.22	+0.41	-23.25	+0.04	+0.23
1612+261	12 08.	1	0.131	16.00	16.26	*	TON 256	-23.53	+0.03	+0.23	-23.47	0.13	40.0
1613+658	16 13 36.3	+65 50 38	0.129	15.37	16.52	•	M	-23.69	4 6	+0.20	-24.07	מ מ מ מ מ	
1626+554	26 51.	24	0.133	16.17	16.44	e o		-23.40	+0.14	+0.33	-23.34	0.01	+0.15
1630+377	30 15.		1.471	15.96	16.38		K 433-16	-29.27	-8.65	-9.23	-28.71	-7.67	-8.40
1634+706	21.	3	1.334	14.90	16.52			-30.08	-10.31	-11.22	-29.57	-8.93	-10.00
1700+518	3 8		0.292		16.5/		3F 75	-25.99	75.57	-2.38	-25.83	-2.75	-2.67
1715+535	15 30	P	1.920	16.30	16.37			-29.61	-9.40	-10,12	-28.93	4.07	-8.89
1718+481	18 17.	07	1.084	15.33	16.44			-29.13	-8.34	-8.87	-28.70	-7.64	-8.37
2112+059	12 23	i N	0.466	15.52	16.30			-26.90	-3.96	-3.88	-26.70	-4.08	-4.16
2130+099	9 6	4 6	0.061	14.62	16.30	9 6	951 W7 II	-23.22	77.04		-25.20	2 4	40.4
22144139	14 45	, ic	0,00	14.98	16.17		MK 304	-23.07	40.39	+0.54	-23.04	40.23	+0.39
2233+134	33 39.		0.325	16.04	16.27		· · · · · · · · · · · · · · · · · · ·	-25.54	-1.98	-1.76	-25.40	-2.17	-2.05
2251+113	51 40.	20	0.323	16.25	16.27		PKS	-25.32	-1.71	-1.48	-25.18	-1.89	-1.75
2302+029	02	S :	1.044	16.03	16.13	•	PB 5235	-28.34	-6.66	-6.92	-27.92	-6.20	-6.63
2304+042	80.50		0.042	15.44	16.09	gen	PB 5250	-21.38	11.08	+1.58	/C.12-	2 6	12.57
2344+092	23 44 03.7	+04 31 33	0.432	16.08	16.18		PKS 07:72	-27.23	-4.53	-4.50	-26.94	4.48	-4.62
		:											

TABLE 2
COUNTS OF BQS OBJECTS

			ALL	N	$I_B < -23$
$B_{\rm lim}$	$\begin{array}{c} AREA \\ (deg^2) \end{array}$	n	$\frac{\sigma(< B_{\rm lim})}{(\deg^{-2})}$	n	$\sigma(< B_{\rm lim})$ (\deg^{-2})
14.8	10714	8	0.0007	6	0.0006
15.0	10714	14	0.0013	11	0.0010
15.2	10714	23	0.0021	18	0.0017
15.4	10714	29	0.0027	23	0.0021
15.6	10671	48	0.0045	35	0.0033
15.8	9982	50	0.0050	36	0.0036
16.0	8171	61	0.0075	44	0.0054
16.2	3800	35	0.0092	26	0.0068
16.4	588	8	0.014	8	0.014

IV. OTHER COMPLETE QUASAR SAMPLES

We discuss in this section published surveys of optically selected quasars with confirmed redshifts and measured magnitudes. Our aim is to draw samples from these surveys that are complete within certain limits of redshift and magnitude.

a) The Braccesi Survey

The Braccesi survey (Braccesi, Formiggini, and Gandolfi 1970) contains 175 objects with an ultraviolet excess over an area of 36 deg². Redshifts based on spectra taken by R. Lynds were given for a number of objects, together with multicolor photometry (u, b, v, i) for most objects. The construction of a complete sample from this survey has been discussed by Schmidt (1974a), Green and Schmidt (1978), and Véron and Véron (1982; see Table 1). Based on (U, B, V) photometry given by Braccesi, Lynds, and Sandage (1968), we adopt the photometric transformation

$$B = b + 0.36(b - v) - 0.35.$$
 (5)

Published spectroscopic work is complete to b = 18.4. As the bluest quasars have b - v = -0.1, we adopt a limiting B magnitude for completeness of $B_{\rm lim} = 18.00$.

We list in Table 3 the 18 objects in the complete sample. We have not included object AB 106 = B272 which has narrow emission lines, and which has been classified as an extragalactic H II region (Downes and Margon 1981). Objects AB 47, 91, and 147 have $M_B > -23$ and hence are not quasars in the sense of § III.

b) The Curtis-Schmidt Surveys

The Curtis-Schmidt telescope at Cerro Tololo Inter-American Observatory has produced two objective-prism surveys of quasars: the CTIO survey and the Michigan-Tololo survey.

The CTIO survey has been published and discussed by Osmer and Smith (1980). All candidate quasars found

TABLE 3
COMPLETE QUASAR SAMPLES

Name ^a	z	В	Name ^a	z	В
AB 7	2.07	17.98	UM 18	1.89	17.15
AB 9	1.241	17.20	UM 86	1.96	17.45
AB 29	1.43	17.81	UM 294	1.92	17.95
AB 47	0.221	17.73	UM 402	2.84	17.95
AB 62	0.28	17.92			
AB 78	1.375	17.13			
AB 84	0.69	17.74	HS 7	2.10	19.15
AB 87	0.78	17.70	HS 9	2.33	18.79
AB 89	1.20	17.97	HS 26	3.45	19.25
AB 91	0.095	17.48	HS 31	2.20	18.57
AB 122	0.490	17.62	HS 34	2.17	19.36
AB 133	0.184	17.16	HS 36	1.86	19.21
AB 141	0.92	17.83	HS 45	2.24	19.47
AB 142	0.30	17.94	HS 46	2.03	19.04
AB 147	0.19	17.88	HS 48	2.04	18.64
AB 154	2.09	17.77	HS 49	1.84	19.10
AB 162	1.75	17.73	HS 54	1.83	18.50
AB 163	0.54	17.41	HS 56	1.86	18.61
			HS 60	2.16	19.46
CT 8	3.16	17.91	HS 62	2.39	19.30
CT 31	2.61	17.93	115 02	2.07	17.00
CT 54	2.76	17.76			
CT 85	2.19	16.97	CXX 16	1.00	18.65
CT 89	3.02	17.79	SW 16	1.82	19.45
CT 93	2.87	17.97	SW 26	2.48	
CT 95	2.41	17.70	SW 35	2.82	19.35 19.35
CT 96	2.80	17.86	SW 76	2.40	18.05
CT 98	2.00	- 17.93	SW 77	2.52	18.03
CT 105	2.29	17.68			
CT 106	1.97	17.83			
CT 108	3.06	18.00	KC 22 ^b	1.74::	19.58
CT 110	2.42	17.50	KC 6B7	2.30	20.74
CT 113	3.23	17.72	KC F5 ^b	1.83::	20.94
CT 115	1.96	17.73	KC 18	3.07	19.56

^aAB refers to the Braccesi sample; CT and UM, to the Curtis-Schmidt samples, from the CTIO survey and the University of Michigan survey, respectively; HS and SW, to the 4 m grating prism surveys, from the Hoag-Smith survey and the Sramek-Weedman survey, respectively; KC, to the Kron-Chiu sample.

^bThe redshift given is based on the arbitrary identification of the single observed emission line as C IV. Different values of the redshift will result if the line is identified as Lyα or Mg II emission; see Fig. 3.

on the objective-prism exposures on IIIa-J emulsion were subsequently observed with slit spectra. The spectral coverage is from approximately 3400 to 5400 Å, corresponding to the redshift range 1.80-3.44 for the Ly α emission line. Since Ly α is the strongest emission line in quasar spectra, we concentrate on quasars from this survey with z > 1.8 as these are most likely to form a complete sample.

Measured fluxes refer to the continuum at an observed wavelength corresponding to 1475 Å in the rest frame. The magnitude $m_{\nu}(1475)$ was defined as

$$m_{\nu}(1475) = -2.5 \log f_{\nu} - 48.59,$$
 (6)

358

where f_{ν} is the flux in ergs s⁻¹ cm⁻² Hz⁻¹ measured at 1475 Å rest wavelength, i.e., $f_{\nu} = f_{\nu}[1475(1+z)]$. Using equation (3), we find

$$B = m_{\nu} (1475) + 0.23 + 1.25 \log 1475 (1+z) / 4400.$$

(7)

The distribution of the magnitude $m_{\nu}(1475)$ shows a peak at 18.5 (Osmer and Smith 1980). Since the magnitude distribution of quasars found in the CTIO 4 m survey shows a peak at 19.5 (Osmer 1980), the peak for the Curtis-Schmidt survey has to be caused by the onset of incompleteness. We assume that the sample is complete to B=18.00; this corresponds to $m_{\nu}(1475)=17.80$ for z=1.8, and $m_{\nu}(1475)=17.61$ for z=3. We list in Table 3 the 15 objects with z>1.8, B<18.00 over the survey area of 340 deg².

Even with this conservative assumption about the limiting magnitude for completeness, we find in fitting models of quasar evolution (see § VII) that these predict more objects than are observed by substantial factors. This had been foreseen by Osmer (1980), who noticed that in the magnitude range of overlap between the CTIO 4 m survey and the Curtis-Schmidt survey there was a large systematic difference in the surface densities, in the sense that the Schmidt results are low.

Osmer (1981) has noted that all the Curtis-Schmidt fields exposed during the second of three runs had low yields of quasars. Dr. Osmer kindly communicated to us which quasars were found in these "suspect" fields. Among the 15 fields in total, there are seven suspect fields which yielded nine quasars with B < 18. The other eight fields produced eight such quasars. It appears, then, that within the adopted completeness limit B = 18 there is no discernible difference between the yields in different runs.

The Curtis-Schmidt telescope has also been used for an objective-prism survey by a University of Michigan group (see Lewis, MacAlpine, and Weedman 1979). The survey covered 392 square degrees. Slit spectra are available for 48% of the quasar candidates found, yielding a list of 68 confirmed quasars given in Table 1 of Lewis, MacAlpine, and Weedman (1979). Magnitudes m_{4500} given are photoelectrically determined continuum magnitudes at 4500 Å in the observer's frame (see Table 3 of Vaucher and Weedman 1980) based on standard stars used by Oke (1974). From equations (1) and (3) we find

$$B = m(4500) + 0.25. (8)$$

Magnitudes m(4500) are given for 51 of the 68 quasars in Table 1 of Lewis, MacAlpine, and Weedman (1979). Among these, four quasars have z > 1.8 and B < 18 (see Table 3). If the selection of candidate objects chosen for spectral analysis and for photometry was independent of redshift and magnitude, then this sample corresponds to an area of 36% of the total survey, or 140 deg².

c) The 4-Meter Telescope Transmission Grating Prism Surveys

The 4 m telescopes at Kitt Peak and Cerro Tololo have been used with transmission grating-prism combinations to produce quasar surveys based on slitless spectra.

Hoag and Smith (1977) used IIIa-F plates at the CTIO 4 m telescope to produce 71 quasar candidates in an area of 5.1 deg². Osmer (1980) obtained slit spectra of all candidates. The magnitudes m_{ν} (1475) measured by Osmer refer to the continuum flux at 1475 Å in the frame of the quasar, defined in equation (6). The magnitude distribution of confirmed quasars with 1.8 < z < 2.5shows a peak at $m_{y}(1475) = 19.5$ (Osmer 1980). The possibility cannot be excluded that the luminosity function in this range of redshift shows a maximum at an absolute magnitude corresponding to $m_{\nu}(1475) = 19.5$. We consider it more likely that the maximum is caused by the onset of incompleteness of the survey. We assume that the sample is complete to B = 19.5; this corresponds to $m_{\nu}(1475) = 19.30$ at z = 1.8, and $m_{\nu}(1475) = 19.11$ for z = 3. We list in Table 3 the set of 14 quasars with z > 1.8, B < 19.50 in the 4 m Tololo survey area of 5.1

Sramek and Weedman (1978) have used the same technique at the Kitt Peak 4 m telescope to survey for faint quasars. They used IIIa-J emulsion, allowing Ly α detection up to a redshift of 3.3. Magnitudes m(4500)and redshifts based on slit spectra were obtained by Vaucher and Weedman (1980) for 53 of the Sramek-Weedman quasar candidates in a total area of 2.7 deg². We use equation (8) to convert m(4500) to a B magnitude. No redshifts are given for four objects with B <19.5. On the basis of spectral coverage and equivalent widths, we expect that objects 12 and 66 have redshifts less than 1.8. Sargent, Young, and Schneider (1982) find z = 2.518 for object 77 and z = 2.605 for object 78. They also noted that object 78 is very close to a much brighter star; we adopt their magnitude m(4500) = 19.4, which makes it fainter than the limiting magnitude B = 19.5.

We list in Table 3 the sample of five quasars with z > 1.8, B < 19.5 in the 4 m Kitt Peak survey area of 2.7 deg². (We omitted No. 18 = KP 1228.7+07.7 which was used as a field center in the Sramek-Weedman survey.) Considering the small numbers, the surface density of 1.9 deg⁻² is in reasonable agreement with that of 2.7 deg⁻² from the 4 m Tololo survey.

d) Selected Area 57

Kron and Chiu (1981) have surveyed the field of Selected Area 57 for faint quasars. In searching for candidates they used as a prime criterion lack of proper motion, based on a proper-motion catalog by Chiu (1980). In addition, they used data from a transmission grating-prism survey of S.A. 57 by A. Hoag and A.

Sandage, a variability study, and multiband photometry. Accurate proper motions in Chiu's (1980) catalog, based on a time span of 25 years, are limited to a radius of 9'. Within that area, all candidates with B < 21 have been studied with slit spectra, yielding the four quasars listed in Table 3. The corresponding surface density of 57 deg⁻² is within the uncertainties consistent with Kron and Chiu's result of 80 deg^{-2} for J < 21.

V. QUASAR COUNTS AND THE DISTANCE SCALE

In this section we present evidence based on quasar counts which, quite apart from the observed redshifts, points to a distance scale for quasars of the same order as the radius of the universe.

Initially, we assume hypothetically that quasars are at cosmologically small distances and test for uniformity of the space distribution of objects by performing the $V/V_{\rm max}$ test (Schmidt 1968). In Euclidean space we have simply

$$V/V_{\text{max}} = \text{dex} \left[0.6(B - B_{\text{lim}}) \right]. \tag{9}$$

We give in Table 4 mean values of $V/V_{\rm max}$ for the entire sample of objects in the BQS, as well as for subsamples obeying $M' < M'_{\rm lim}$, where

$$M' = B - 5 \log z - 43.89. \tag{10}$$

M' is approximately the absolute magnitude of a quasar in case the redshift is cosmological. However, in our present context we use M' merely as a label, derived from observed quantities B and z. For objects with a uniform space distribution, the quantity $\sigma = (12n)^{-1/2}$ is the standard deviation from the value 0.50 (Rowan-Robinson 1970).

All values of $\langle V/V_{\rm max} \rangle$ given are larger than the value 0.50 corresponding to a uniform distribution in space, by 3-4 σ . The second entry is probably the most appropriate one, since in the cosmological context we concentrate in this paper on quasars with $M_B < -23$ (see § III).

We can obtain, within the context of the local hypothesis, an entirely independent check on the uniformity from the slope of the counts obtained by comparing the total content of the BQS and the Braccesi survey.

TABLE 4
EUCLIDEAN V/V_{max} VALUES FOR
BOS QUASARS

$M'_{\rm lim}$	n	$\langle V/V_{\rm max} \rangle$
	114	0.587 ± 0.027
−23	92	0.613 ± 0.030
−24	69	0.654 ± 0.035
−26	33	0.671 ± 0.050

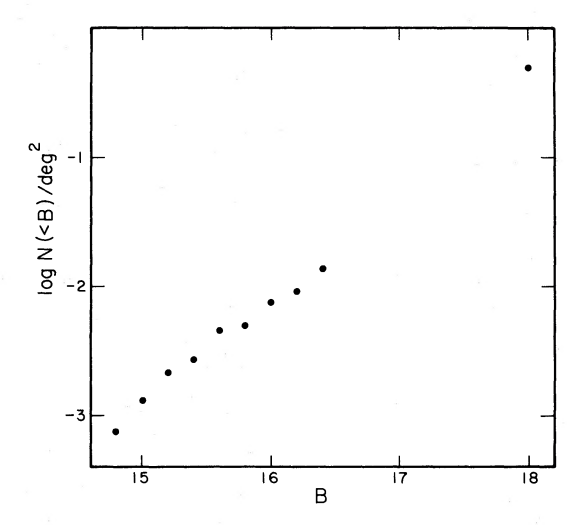


FIG. 2.—Cumulative surface densities, per square degree, for the Bright Quasar Survey ($B \le 16.4$) (see Table 2) and the Braccesi sample (B = 18.0).

Surface densities N(< B) for both surveys are shown in Figure 2 (see also Table 2).

Each of the BQS points can be combined with the Braccesi point to yield a slope $b = d(\log N)/dB$. These slopes range between b = 0.85 and b = 0.96. We adopt $b = 0.90 \pm 0.05$, where the standard deviation is consistent with the number of objects counted. This result is essentially identical to that obtained earlier (Green and Schmidt 1978) from preliminary results for a small part of the BQS.

The slope derived is significantly larger than the value b=0.60 corresponding to a uniform distribution in Euclidean space. We would have obtained a larger value yet if we had limited the counts to objects with M' < -23. The limit z < 2.15 applying to each of the two surveys has the effect of decreasing the measured slope since, empirically, the redshift increases on the average with apparent magnitude.

If, for illustration, we assume that the space density is a power law r^n of distance r, then the slope b = 0.90 corresponds to n = 1.5 (and to $V/V_{\text{max}} = 0.60$). If quasars were local, their density would have to increase by a factor of 1000 for an increase of distance by a factor of 100.

Apparently, we would be located in a deep density minimum in the assembly of quasars. This situation would only be acceptable in the local hypothesis advanced by Terrell (1964) in which quasars are ejected by our Galaxy. In other versions of the local hypothesis, the special location imposed on us is an embarrassment since other cosmic observers elsewhere would have to see different quasar counts. Therefore, we believe on such Copernican grounds that these local hypotheses of quasars are to be rejected.

360

Fig. 3.—Hubble diagram for complete samples drawn from five surveys of optically selected quasars (see Tables 1 and 3). The line corresponds to absolute magnitude $M_B = -23$.

17 В

14

15

The Copernican argument just discussed applies equally for distances of 1 Mpc or of 100 Mpc. It breaks down only when the distances to quasars are so large that their light travel time is a substantial fraction of the age of the universe. In that case, counts to different depths refer to objects observed at different cosmic times and hence cosmological evolution can affect count slopes and V/V_{max} . We are released from the Copernican restraint at a distance scale which is essentially the same as that corresponding to the cosmological interpretation of the observed large redshifts.

VI. PROCEDURE FOR DERIVATION OF EVOLUTION AND LUMINOSITY FUNCTIONS

We show in Figure 3 the Hubble diagram of the 174 quasars that belong to the complete samples discussed above. It should be remembered that the BQS has a distribution of limiting B magnitudes ranging from 15.46 to 16.63. The adopted redshift and magnitude limits for

the other samples, listed in Table 6, are easily recognized in Figure 3.

We are interested in deriving the space density of quasars as a function of their absolute magnitude M_B and redshift z, i.e., the luminosity function $\Phi(M_B, z)$. The absolute magnitude M_B is related to apparent magnitude B and redshift z by

$$M_B = B - 5 \log A(z) + 2.5(1 + \alpha) \log (1 + z) - 43.89,$$
(11)

where we use a Hubble constant $H_0 = 50 \text{ km s}^{-1} \text{ Mpc}^{-1}$. The quantity A(z) is the bolometric luminosity distance, since observed bolometric flux is proportional to A^{-2} . We use for A an expression given by Terrell (1977):

$$A(z) = z \left\{ 1 + \frac{z(1 - q_0)}{\left[(1 + 2q_0 z)^{1/2} + 1 + q_0 z \right]} \right\}$$
 (12)

which is valid for $q_0 \ge 0$. This expression was obtained by transforming a formula given by Mattig (1958) which for small values of q_0z is difficult to evaluate numerically, as discussed by Terrell. The term $2.5(1+\alpha)\log(1+z)$ in equation (11) reflects the effect of the redshift on measurements through a fixed color band.

If we had available the Hubble diagram for all quasars in the sky, then the luminosity function at redshift z would be simply reflected by the distribution of quasars in a horizontal slice at redshift z:

$$n(B,z) dB dz = \Phi(M_B,z) dM_B dV, \qquad (13)$$

where dV is the comoving volume of the universe in the redshift range z to z + dz.

In practice, we are far from having full coverage of the quasar Hubble diagram. In particular, as shown in Figure 3, we almost completely lack information for B > 18, z < 1.8. As a consequence, at redshifts below 1.8 only a short stretch of the luminosity function can be determined directly, through equation (13). In order to make progress in this situation, we are forced to make some assumption about the luminosity function $\Phi(M_B, z)$, in particular about its dependence on z. This redshift dependence is usually referred to as evolution.

Pure density evolution is based on the assumption that evolution is independent of M_B , i.e.,

$$\Phi(M_B, z) = \Phi(M_B, 0)\rho(z) \tag{14}$$

where $\Phi(M_B,0)$ is the local luminosity function. This case was initially adopted for the evolution of quasi-stellar radio sources (Schmidt 1968) and optically selected quasars (Schmidt 1970). Evidence discussed in the next section shows that this assumption cannot be maintained.

Pure luminosity evolution keeps the luminosity function constant, both in shape and numbers, but allows a shift of the luminosity coordinate as a function of redshift:

$$\Phi\left[M_B + L(z), z\right] = \Phi(M_B, 0). \tag{15}$$

This case would apply, for instance, to an assembly of objects of different luminosities that are all experiencing the same evolution L(z), or L(t), in their luminosity (in magnitudes). This case was introduced for galaxy evolution by Sandage (1961) and for quasar evolution by Mathez (1978). We will discuss some aspects of pure luminosity evolution in Appendix C.

In selecting an evolution law for quasars, we were guided by two pieces of evidence. First, $\langle V/V_{\rm max} \rangle$ values for the BQS show a strong dependence on M_B (see Table 7). For the most luminous quasars $\langle V/V_{\rm max} \rangle$ is almost 0.8, while for the least luminous ones it is around 0.5. Second, we can determine $\Phi(M_B, z)$ for a given M_B at different redshifts from equation (13) in selected

regions of the Hubble diagram that are covered by surveys (see Fig. 3). The z-dependence of the $\Phi(M_B,z)$ values so determined turns out to be steeper for more luminous quasars, confirming the trend indicated by $\langle V/V_{\rm max} \rangle$ for the BQS.

Guided by the above evidence, we assume that the comoving space density of quasars of given M_B is an exponential function of cosmic time, with a coefficient in the exponential depending linearly on M_B , i.e.,

$$\Phi(M_B, z) = \Phi(M_B, 0) \exp\left[k(M_0 - M_B)\tau(z)\right],$$
(16)

where k and M_0 are constants, and $\tau(z)$ is the light travel time, expressed as a fraction of the age of the universe. We assume that k = 0 for $M_B > M_0$, i.e., we do not admit evolution of a different sign for low-luminosity objects.

The exponential dependence of density on cosmic time was first proposed by Rowan-Robinson (1970). There is a general impression that this is a reasonable approximation, but the evidence will remain weak until larger parts of the Hubble diagram of quasars are covered by surveys suitable for statistics. This also applies to the luminosity dependence of the coefficient of cosmic time in the density law, which is simply assumed to be linear with M_R for lack of better evidence.

Since the BQS covers the entire range of absolute magnitudes, we will use it to derive the local luminosity function $\Phi(M_B,0)$ for assumed values of k and M_0 . These are then used to predict the content of the other complete samples. The model fitting procedure consists of varying the values of K and M_0 until a satisfactory fit is obtained.

The local luminosity function $\Phi(M_B,0)$ is made up of discrete contributions from each of the *n* objects in the complete sample used for its derivation (Schmidt 1968), in this case the BQS:

$$\Phi(M_B,0) = \sum_{j=1}^{n} (V_a')_j^{-1} \delta(M_{B_j} - M_B), \qquad (17)$$

where V'_a is the density-weighted accessible volume (Avni and Bahcall 1980). The accessible volume V_a is the total comoving volume of the universe within which a given quasar is observable within the limits of the complete sample. V'_a is the density-weighted equivalent of V_a .

The BQS covers 266 separate fields which exhibit 74 different limiting magnitudes $B_{\lim,i}$, each valid over ω_i steradians. The density-weighted accessible volume V'_a for one quasar belonging to the BQS is

$$V_a' = \sum_i \frac{\omega_i}{4\pi} \int_0^{z_{\text{max},i}} \rho(z) (dV/dz) dz, \qquad (18)$$

where, by assumption,

$$\rho = \exp\left[k(M_0 - M_B)\tau(z)\right]. \tag{19}$$

The value of z_{max} is determined from

$$B_{\lim, i} - 5 \log A(z_{\max, i}) + 2.5(1 + \alpha)$$

 $\times \log (1 + z_{\max, i}) - 43.89 = M_B$ (20)

(see eqs. [11] and [12]). The volume element is

$$\frac{dV}{dz} = 2709 \frac{A^2}{(1+z)^2 \left[A^2 (1-2q_0) + (1+z)^2\right]^{1/2}} \times \left[\frac{1}{q_0} + \left(1 - \frac{1}{q_0}\right) (1+2q_0z)^{-1/2} - \frac{A}{(1+z)}\right]$$
(21)

in $\mathrm{Gpc^3}$ for $H_0 = 50 \mathrm{~km~s^{-1}~Mpc^{-1}}$, for $0 < q_0 \le 0.5$. The light travel time, expressed as a fraction of the age of the universe, is (see Sandage 1961)

$$\tau = 1 - (1+z)^{-3/2}$$
 for $q_0 = 0.5$,
 $\tau = 1 - g(z)/g(0)$ for $0 < q_0 < 0.5$, (22)

where

$$g(z) = a(z) - 1/a(z) - 2\ln a(z),$$

$$a(z) = \frac{q_0^{-1} - 1 + z}{1 + z} + \left[\frac{\left(q_0^{-1} - 1 + z\right)^2}{\left(1 + z\right)^2} - 1 \right]^{1/2}.$$

The number of quasars predicted to belong to a given survey can be written as

$$N(\text{survey}) = \sum_{n} \frac{V'(\text{survey})}{V'_{a}}, \qquad (23)$$

where n is the total number of quasars in the BQS sample, V'(survey) is the accessible density-weighted volume in the survey for a given BQS quasar, and V'_a its accessible density-weighted volume in the BQS itself (eq. [18]).

In particular, we can derive the number of quasars expected with redshifts in the range z_1-z_2 and magnitudes B_1-B_2 in solid angle ω as

$$N(z_1, z_2; B_1, B_2) = \sum_{n} \frac{V'}{V'_a},$$
 (24)

where

$$V' = \frac{\omega}{4\pi} \int \rho(z) \left(\frac{dV}{dz}\right) dz, \qquad (25)$$

where the integration is from max $[z_1, z(B_1)]$ to

 $\min [z_2, z(B_2)]$, and where V'_a is given in equation (18), and $z(B_2)$ by

$$M_B = B_2 - 5 \log A[z(B_2)]$$

 $+ 2.5(1 + \alpha) \log [1 + z(B_2)] - 43.89.$ (26)

VII. MODELS OF QUASAR EVOLUTION AND LUMINOSITY FUNCTIONS

The procedure described in the preceding section will yield a local luminosity function that, by construction, fits the BQS for any given density law. Since the adopted density law (see eq. [19]) contains two free parameters, k and M_0 , we can set their values such that the total numbers of two further samples are represented. For this purpose we use the 4 m transmission grating prism sample and the Kron-Chiu sample in S.A. 57. These two samples are most separated in magnitude (and hence in redshift for given M_B) from the BQS, allowing the most reliable determination of the density increase.

The sample of only four faint quasars in S.A. 57 is statistically very weak. In addition, for two of the objects only one emission line has been detected. The redshifts plotted in Figure 3 correspond to identification as C IV emission, with arrows pointing to redshifts corresponding to alternative identifications as Ly α or Mg II emission. In the latter case, the absolute magnitude of one or both (depending on q_0) is fainter than -23, leaving only two or three quasars in the sample. Under these circumstances we have decided to adopt two alternative values for N(B < 21, z < 3.1), namely a high value (H) of 60 deg⁻², and a low value (L) of 30 deg⁻².

We use for the BQS and the Braccesi sample an upper redshift limit of 2.15; at larger redshifts the ultraviolet excess on which these samples are based may disappear due to the appearance of Ly α emission in the B filter. Neither of these surveys contains, in fact, any quasars with z > 2.15. The redshift limit 2.15 will replace $z_{\rm max}$ determined from equation (20) whenever the latter exceeds 2.15.

Since there is strong evidence that the increase in space density does not persist beyond redshift 3.5, we have fitted our models to a redshift z_{lim} well below redshift 3.5. These models will then be extrapolated to redshifts beyond 3.5 for comparison with the observations (see § IX). We chose $z_{lim} = 3.1$ based on a casual inspection of the redshift distribution of Curtis-Schmidt quasars. The results are probably little affected by this choice, since there is no clear evidence for a break in the density increase out to z = 3.5 (see § IX). We give in Table 6 the surface densities for quasars with z < 3.1 and $M_B < -23$ in the surveys under discussion.

We have determined the values of k and M_0 by trial and error for two alternative Friedmann models of the

TABLE 5 Local Luminosity Function $\Phi(M_B(0),0)$ for Four Evolution Models^a

		Mo	DEL	
PARAMETER	HH1	HLI	HH5	HL5
90	0.1	0.1	0.5	0.5
\widetilde{M}_0	-21.87	-23.26	-20.12	-22.01
k	3.13	4.19	2.18	3.14
	30°	Lo	од Ф	*
M_R :				
- 30.5	-10.12	-11.08		
−29.5	-7.84	-8.41	-8.01	-8.97
-28.5	-5.97	-6.23	-5.88	-6.40
−27.5	-3.79	-3.75	-4.46	-4.64
-26.5	-1.89	-1.71	-2.32	-2.29
-25.5	-0.65	-0.42	-1.15	-1.04
-24.5	0.52	0.74	0.33	0.50
- 24.3	0.52	0.74		

^aListed is $\log \Phi$, where Φ is the number per comoving $\mathrm{Gpc^3}$ per magnitude for $H_0 = 50 \mathrm{~km~s^{-1}~Mpc^{-1}}$.

 ${\bf TABLE~6}$ Observed and Predicted Surface Densities for Four Surveys

						σ (deg	⁻²)		
							Model	3	
SURVEY	z .	$B_{\rm lim}$	n	Observed	NE1	HHI	HL1	HH5	HL5
Braccesi	0-2.15	18.0	15	0.42	0.06	0.35	0.30	0.41	0.36
Curtis-Schmidt	1.8-3.1	18.0	17	0.035	0.003	0.14	0.17	0.065	0.08
4 m grating prism	. 1.8-3.1	19.5	18	2.3	0.01	2.3	2.3	2.3	2.3
Kron, Chiu	. 0-3.1	21.0	4	57	1.0	61	30	60	31

universe, with deceleration constant³ $q_0 = 0.1$ and 0.5, respectively; and for N(B < 21, z < 3.1) = 60 and 30 deg⁻², respectively. These models, coded HH1, HL1, HH5, and HL5, are listed in Table 5. The first letter (H) indicates the high surface density adopted for the 4 m transmission grating prism surveys.⁴

In all cases, k turned out to be positive; i.e., evolution is steeper for more luminous quasars. The value of M_0 , which is the luminosity for which evolution is zero, ranges from approximately -23 to -20, close to the adopted lower limit of quasar luminosity (§ III). The evolution is very strong: e.g., in model HH1 the e-folding time of the density increase is 10% of the age of the universe for $M_B = -25$, and only 5% for $M_B = -28$.

⁴Appendix A presents models based on an alternative, low surface density for the 4 m grating prism surveys.

The values of $(V_a')^{-1}$ for each of the BQS objects in each of the four models are listed in Table 1, in units of inverse comoving volume of 1 Gpc³. We give in Table 5 the local luminosity function $\Phi(M_B,0)$ obtained by binning⁵ the individual $(V_a')^{-1}$ values (see eq. [17]).

Table 6 shows the predicted surface densities for the evolution models. The fit to the Braccesi survey is well within its statistical uncertainty. Predicted numbers for the Curtis-Schmidt surveys are higher than the observed numbers by a factor between 2 and 5. Osmer (1980) had noted that the Curtis-Schmidt numbers seemed low compared to those of the 4 m surveys. It should be noted that the quasars in the Curtis-Schmidt surveys are more luminous than those of the 4 m surveys. Part of the observed discrepancy could be explained if the evolution of the most luminous quasars does not steepen with luminosity.

 $^{^3}$ Considering the present day uncertainty in the value of q_0 , our choice of 0.1 is rather arbitrary. We did want to avoid the case of an empty universe, $q_0 = 0$ (assuming zero universal constant), since q_0 is presumably greater than 0, and since the geometry changes rather rapidly with q_0 at small values of q_0 .

⁵We have used in this paper exclusively individual $(V_a')^{-1}$ values. The binned luminosity functions $\Phi(M_B,0)$ and $\Phi(M_B,z)$ (see Fig. 4) are given for illustration.

SCHMIDT AND GREEN

		$M_B(q_0)$	= 0.1)	
PARAMETER	-30.626	-2624	-2423	-23-20.7
No evolution:				
$\langle V_e/V_a\rangle \dots$	0.76	0.62	0.49	0.50
$\langle V/V_{\text{max}} \rangle \dots$	0.78	0.66	0.51	0.49
Evolution model HH1:				
$\langle V'_{e}/V'_{a}\rangle \dots$	0.48	0.49	0.45	0.49
$\langle V'/V'_{\text{max}} \rangle \dots$	0.54	0.55	0.47	0.48
n	36	33	23	22
σ	+0.05	+0.05	± 0.06	+0.06

Table 6 also shows predicted numbers (NE1) for the case k = 0, i.e., no evolution, derived following the same procedure used for the evolution models. The effect of evolution is dramatically illustrated.

So far, we have not used $V/V_{\rm max}$ or density-weighted $V'/V'_{\rm max}$ values (Schmidt 1968) for the BQS to study evolution. The reason is that coupling the BQS with the other complete samples provides more leverage (i.e., larger range of τ for given M_B) than can be obtained within the BQS itself. Nonetheless, it is of interest to look for evidence of evolution internal to the BQS.

In deriving V'/V'_{max} values for quasars in the BQS, we use the limiting magnitude B_{lim} that applies at the position of each individual object (see Table 1). Since B_{lim} is different in different directions, the density-weighted volumes V' and V'_{max} refer essentially to vanishingly small pencil beams around each quasar. Avni and Bahcall (1980) have suggested the use of an alternative estimator, V'_e/V'_a , for surveys in which limits are different in different directions. The accessible volume V'_a has been defined in the preceding section and equation (18). V'_e is the density-weighted volume out to redshift z, or to $z_{\text{max},i}$ if it is smaller than z:

$$V_e' = \sum_i \frac{\omega_i}{4\pi} \int \rho(z) (dV/dz) dz, \qquad (27)$$

where the integration is from 0 to min $(z; z_{\max, i})$.

We show in Table 7 values of $\langle V/V_{\rm max} \rangle$ and $\langle V_e/V_a \rangle$ for BQS quasars in different ranges of absolute magnitude for the case $q_0=0.1$. Also shown are the density-weighted values $\langle V'/V'_{\rm max} \rangle$ and $\langle V'_e/V'_a \rangle$ for model HH1. If the density laws used are correct, then the quantity $\sigma=(12n)^{-1/2}$ given in Table 7 is the standard deviation of $\langle V'/V'_{\rm max} \rangle$ or $\langle V'_e/V'_a \rangle$ from the value 0.50 (Rowan-Robinson 1970). Even though model HH1 was derived by linking the BQS with other surveys, it appears to be successful in yielding $\langle V'_e/V'_a \rangle$ and $\langle V'/V'_{\rm max} \rangle$ values that are statistically compatible with the value 0.5. This is the case for all models given in Table 5 as well as those discussed in Appendix A.

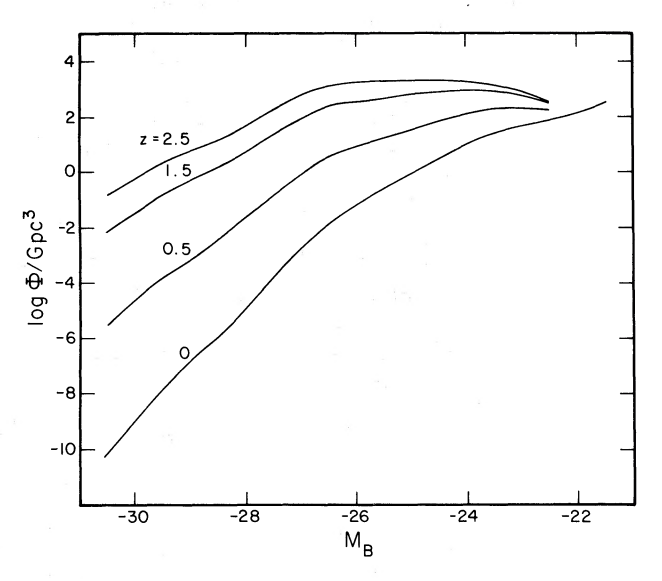


FIG. 4.—Luminosity functions $\Phi(M_B, z)$ per magnitude per comoving volume unit of 1 Gpc³ for model HH1. The slight waviness is caused by statistical fluctuations in the data used for the derivation (see text). At each redshift only part of the luminosity function is actually covered by data from existing surveys. Objects with $M_B > -23$ are mostly Seyfert nuclei (see Appendix B).

The luminosity function $\Phi(M_B, z)$ can be obtained at any redshift from the data in Table 5 and equation (16). We illustrate in Figure 4 the luminosity function for model HH1 at various redshifts. As a consequence of the luminosity-dependent density increase, the luminosity function becomes flatter for larger redshifts. It should be stressed that these luminosity functions represent models, and that parts of each luminosity function given are not covered by direct observational evidence at present. In addition, the bright end of the luminosity function at small redshift is unobservable, in principle, because the universe lacks sufficient volume out to small redshifts to yield a single object.

TABLE 8 Redshift-Magnitude Table $^{\rm 4}$ for Model HH1 (see Table 5)

AB(6500) 13.55		14.55	*	15.55		16.55	17.55	5	18.55	19.55		20.55 21	21.55 22	22.55	- 4	23.55 24	24.55
P1 q		:															
$z = 5.0 \dots$	0.0000		0.0000	,	0.0000	0.	0.017	0.11		1.3	1.8	73	20	81	73	57	
$z = 4.5 \dots$	0.0000		0.0000	J	0.0000	0.	0.015	0.17		1.2	5.9	i i	35	57	67	39	
$z = 4.0 \dots$	0.0000		0.0000		0.0010	0	0.021	0.21		8.0	7.5	4	45	45	20	21	
z = 3.5	0.0000		0.0000		0.0035	0	0.031	0.36		8.0	8.4	3	37	41	37	9	
$z = 3.0 \dots$	0.0000		0.0000	_	0.0030	0	0.040	0.24		2.2	15.8	2	23	32	20	0	_
z = 2.5	0.0000		0.0004	_	0.0047	0	0.061	0.24		2.5	13.3	_	18	21	2)	
$z = 2.0 \dots$	0.0000		0.0003		0.0058	0	0.032	0.47		4.4	7.3	,	12	∞ ′	0)	-
z = 1.5	0.0000		0.0005	-	0.0049	0	0.065	0.82		2.2	5.0		5	0	0	O	_
z = 1.0	0.0000		0.0005		0.0118	0	0.123	0.46		1.3	1.3		0	0	0)	0
z = 0.5	0.0007		0.0038		0.0181	0	0.062	0.12		0.0	0.0		0	0	0	<u> </u>	0
$z = 0.0 \dots$						c	- 317	17.0		13.5	51.1	5	95	101	61	·	, 9
N(z < 3.5)	0.0008		0.0056		0.0517		0.415	2.71									

^aEntries are n(B, z) per sq. deg.

AB(6500) 13.55 B		14.55 15	15.55 16	\$	16.55 17	17.55 18	18.55 19	19.55 20	20.55 21	21.55 22	22.55 23	23.55 24	24.55 25
$z = 5.0 \dots$	0.0000	0.0	0.0000	0.0000	0.028	81.0		2 2	2.1	14	32	=	4
$z = 4.3 \dots$	0.0000	0.0	0.0000	0.0000	0.024	1 0.26		1.6 5	5.5	61	18	∞	2
2 - 4:0	0.0000	0.0	0.0000	0.0015	0.031	0.30		1.1 6	6.5	21	10	5	1
3.0	0.0000	0.0	0.0000	0.0050	0.043	0.49		9 6.0	6.1	16	7	3	0
2 – 3.0	0.0000	0.0	0.0000	0.0039	0.053	0.31		2.0 8	8.4	7	4	_	0
	0.0000	0.000	900	0.0055	0.076	0.25		9 6.1	6.2	4	2	0	0
$z = z.0 \dots$	0.0000	0.000	903	0.0065	0.037	0.42		2.5 2.	2.3	2	_	0	0
	0.0000	0.000	900	0.0053	0.061	0.54		1.0	1.1	-	0	0	0
z – 1.0	0.0000	0.000	002	0.0107	0.090	0.23		0.4 0.	0.2	0	0	0	0
	0.0008	0.0038	038	0.0147	0.038	0.05		0.0	0.0	0	0	0	0
N(z < 3.5)	0.0000	0.00	0.0056	0.0517	0.398	2.28		8.6 24.3		29	14	4	0

^aEntries are n(B, z) per sq. deg.

TABLE 10

REDSHIFT-MAGNITUDE TABLE^a FOR MODEL HH5 (see Table 5)

AB(6500) 13.55 B 14		14.55 15		15.55 16	16.55 17	17.55		18.55 19	19.55	20.55 21		21.55 22	22.55 23	55	23.55 24	24.55 25
$z = 5.0 \dots$	0.0000		0.0000	0.0000	0	0.004	0.04	0.1		2.0	12	33	* - <u>-</u>	49	, E	
$z = 4.5 \dots$	0.0000	<u> </u>	0.0000	0.0006	9	900.0	0.08	0.4		4.4	4	36		42	0	
$z = 4.0 \dots$	0.0000)	0.0000	0.0013	3	0.011	0.07	9.0		7.1	17	38		30	0	
$z = 3.5 \dots$	0.0000)	0.0000	0.0012	2	0.013	90.0	0.7		8.2	19	43		14	0	
$z = 3.0 \dots$	0.0000)	0.0001	0.0020	0	0.024	0.12	1.7		8.1	25	37		-	0	
$z = 2.5 \dots$	0.0000)	0.0003	0.0032	2	0.022	0.24	3.5		9.2	25	20		0	0	
$z = 7.0 \dots$	0.0000)	0.0003	0.0050	0	0.030	0.50	3.2		11.4	22	2	•	0	0 1	
Z = 1.5	0.0000)	0.0005	0.0038	∞	0.068	0.90	3.4		10.1	5	0		0	0	
$z = 1.0 \dots$	0.0000	J	9000.0	0.0132	2	0.157	0.79	2.7		2.0	0	0		0	0	
$z = 0.5 \dots z$ $z = 0.0 \dots$	90000)	0.0038	0.0216	, 9	0.095	0.21	0.0		0.0	0	0		0	0	
N(z < 3.5)	0.0007	٠	0.0056	0.0501	_	0.410	2.84	15.2		49.0	16	102		15	0	

^aEntries are n(B, z) per sq. deg.

 $\label{eq:table-1} {\sc Table 11}$ Redshift-Magnitude Table 5)

AB(6500) 13.55 B 14	13.55 14	14.55		15.55 16	16.55	17.55		18.55	19.55	20.55	21.55	22.55	23.55	24.55 25
$z = 5.0 \dots$	0.0	0.0000	0.0000	0.0000		0.007	90:0	0.2	- 2	2.1	∞	01	9	0
z = 4.5	0.0	0.0000	0.0000	0.0010	0	0.010	0.12	0.5	κi	3.9	∞	6	\$ -	0
$z = 4.0 \dots$	0.0000	000	0.0000	0.0019	0.	0.016	0.10	0.7	5.	5.8	7	∞	3	0
$Z = 5.5 \dots$	0.0000	000	0.0000	0.0017		0.019	0.09	0.8	9		7	∞		0
$z = 5.0 \dots$	0.0	0.0000	0.0001	0.0026		0.034	0.16	1.6	.5	5.3	x 0	5	0	0
$z = z.5 \dots z$	0.0000	000	0.0004	0.0039	0	0.029	0.28	2.9	4	4.4	٠,5	3	0	,
$z = z.0 \dots$	0.0000	000	0.0003	0.0059		0.037	0.49	2.3	4.	4.2	₩.	0	0	0
$\dots \dots $	0.0000	000	0.0005	0.0042	0	0.071	0.75	1.7	2.8	∞		0	0	
	0.0000	900	0.0005	0.0131	0	0.134	0.46	1.0	0.5		0	0	0	-
$z = 0.0 \dots$	0.0006	900	0.0038	0.0187	0.	0.064	0.11	0.0	0.0		0		0	0
N(z < 3.5)	0.0007	207	0.0056	0.0501	0	0.388	2.33	10.3	23.4	4 26		91	7	0

^aEntries are n(B, z) per sq. deg.

VIII. PREDICTED DISTRIBUTIONS OF REDSHIFTS AND MAGNITUDES

We give in Tables 8-11 surface densities n(B,z) for quasars with $M_B < -23$ based on the evolution models HH1, HH5, HL1, and HL5. We give in Appendix A further tables for models LL1 and LH1. These tables may be useful in planning surveys, for the interpretation of data on quasi-stellar radio sources, X-ray quasars, etc.

Detailed inspection of the tables will show irregularities in the distribution of magnitudes at a given redshift. These reflect properties of the BQS, whose individual objects were used in generating models and tables (see § VI)—in particular, the apparent gap in redshifts around 0.8–0.9 seen in Figure 3. We do not have an explanation of this gap in terms of observational selection or bias. The gap may be a statistical fluctuation.

There is evidence (see § IX) that numbers above z = 3.5 are much lower than given by the models. The upper three rows of Tables 8–11 are given for illustration only. At the bottom of the tables are given predicted differential counts n(B) per magnitude interval for z < 3.5. If a different cutoff for quasar redshifts is indicated, revised counts are easily derived. The differential counts show a maximum around B = 21-22. It is easily seen that this maximum is sensitive to the assumed value of the redshift cutoff.

We show in Figure 5 the cumulative counts $N(\cdot < B)$. The dramatic effect of evolution, by factors as large as 100, is seen from the curve NE1 which corresponds to no evolution, for $q_0 = 0.1$.

We have refrained from using data on counts of blue stellar objects since (a) confirmation of the objects as quasi-stellar objects is essential (see Véron and Véron 1982), and (b) the redshifts carry much of the information in the interpretation of quasar statistics. For observational evidence on the faintest quasars, however, we have to contend with counts since the process of taking spectra of these objects is very slow.

Koo and Kron (1982) have counted stellar objects on the basis of photometry in the four bands U, J, F, and N. On the basis of color-color diagrams for 659 stellar objects with B < 22.5 in an area of 1055 arcmin² in Selected Area 68, they selected 65 objects as likely quasars, corresponding to a surface density of 220 deg⁻². We expect on the basis of our models 210 deg⁻² (models HH1 and HH5) to 70 deg⁻² (models HL1 and HL5), both for z < 3.5. Kron (private communication) has found surprisingly few emission-line objects in follow-up spectroscopy and now believes that the surface density must be less than 220 deg⁻².

IX. PREDICTED QUASAR NUMBERS AT REDSHIFTS LARGER THAN 3.5

For many years the suspicion has existed that quasars of very large redshift were rarer than one might expect from their observed numbers at lower redshifts. Initially,

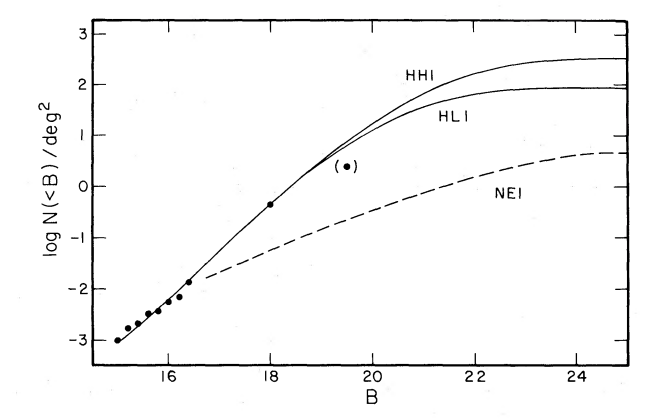


FIG. 5.—Cumulative surface densities, per square degree, for quasars with z < 3.5 and $M_B < -23$. Dots refer to the BQS for $B \le 16.4$ (see Table 2); the Braccesi and Curtis-Schmidt surveys for B = 18.0; and the 4 m grating prism surveys for B = 19.5 (in parentheses since this point refers to 1.8 < z < 3.5 only). The continuous curves refer to evolution models HH1 and HL1, and the dashed curve corresponds to the case of no evolution.

it was suspected that quasi-stellar radio sources might exhibit a redshift cutoff between a redshift 2.5 and 3 (Schmidt 1970, 1972; Sandage 1972). Since the dependence of the radio luminosity function of quasi-stellar radio sources on their optical luminosity (Schmidt 1972) is probably not understood yet, it is preferable to study the redshift distribution of optically selected quasars.

The transmission grating prism survey for quasars with the CTIO 4 m telescope (Hoag and Smith 1977) yielded no redshifts larger than z = 3.45, although the wavelength range covered allowed detection of Ly α emission at redshifts up to 4.7. Carswell and Smith (1978) have shown that the ultraviolet blaze of the grating used for the survey resulted in a reduced sensitivity for redshifts beyond 3.5. As a result, the absence of observed redshifts beyond 3.5 is not in conflict with density evolution as derived from lower redshifts.

Osmer (1982) used a red-blazed grating prism on the CTIO 4 m telescope to survey 5 square degrees for quasars with Ly α emission in the range 3.7 < z < 4.7. He detected emission lines in 15 quasars in the $\lambda\lambda 5700-6900$ bandpass, but in no case was the emission line eventually identified as Ly α . With the evolution models developed in the present paper, we are able to make predictions based on extrapolation of the evolution determined for z < 3.1 into the range 3.7 < z < 4.7. These predictions can then be confronted with Osmer's null result.

Osmer (1982) compared the limiting sensitivity of his survey and the Hoag-Smith survey by considering exposure times and grating efficiencies, as well as by comparing quasar detections with 2.68 < z < 3.45 in the two surveys. He concludes that the new survey reaches 1.2 mag fainter than the Hoag-Smith survey. We adopted

TABLE 12 Expected Number of Quasars over an Area of 5 Deg^2

Lim. Mag.		Mod	EL	
AB(6500)	HHI	HLI	HH5	HL5
20.25	34	39	19	20
19.75	14	20	7	9

for the Hoag-Smith survey a completeness limit of B = 19.5 (see § IV), or AB(6500) = 19.05 (see eq. [4]). Osmer's limit for his survey then corresponds to AB(6500) = 20.25.

We give in Table 12 the predicted numbers of quasars with 3.7 < z < 4.7 over an area of 5 deg², for limiting magnitudes AB(6500) = 20.25 and 19.75. The table shows that predictions range over a factor of 2 for different models. They also show the effect of a change in the adopted limit of completeness. These numbers provide a more solid basis of comparison against which Osmer's (1982) result of zero quasar detections can be judged. Osmer (1982) based his claim for a decrease in the space density of quasars for redshifts larger than 3.5 on extrapolations from the Hoag-Smith survey with an assumed evolution law, which yielded predicted numbers similar to those in Table 12.

It is of interest to check whether the Hoag-Smith survey shows any deficiency of quasars between redshift 3.1 (which was the maximum redshift to which evolution models were fitted) and redshift 3.5. The survey shows one quasar in this redshift range. Our models predict numbers ranging from 1 to 3. Hence, there is no evidence in the Hoag-Smith survey about the redshift at which the deficiency sets in.

X. COMMENTS AND DISCUSSION

The statistical analysis in this paper fully employs the property that each object in a complete sample contributes linearly to the luminosity function. We have, in fact, derived predicted counts for other surveys as a sum of contributions from quasars in the BQS sample (see eqs. [23]–[26]). The advantage of this method is that

there is no need for binning. Binning quasars can be treacherous since their luminosity function is very steep at the bright end. In the case of the BQS, binning would have been impractical since there is a wide distribution of limiting magnitudes $B_{\rm lim}$.

In the derivation of the statistical evolution models, we have fitted only to the total content of surveys other than the BQS, and have not investigated their internal redshift or magnitude distributions. With less than 20 objects per survey, this probably would not have yielded any further significant information.

We have ignored effects due to gravitational lensing, even though PG 1115+08 is a newly detected member of the BQS sample. Turner (1980) initially suggested that lensing might cause substantial apparent statistical evolution in quasars. Subsequent work (Avni 1981; Peacock 1982) shows apparent evolution to be relatively minor if the deamplification of quasars well away from lenses is taken into account.

The main result from the present work is that the increase of quasar space density with redshift depends strongly on absolute luminosity. Detailed information about the variation of the luminosity function with redshift is still lacking. As a consequence, we have to make assumptions about the quasar evolution law which would be unnecessary if there were better coverage of the Hubble diagram by complete quasar samples. Quasar surveys that are complete to B=20 and fainter, covering the entire redshift range, are very much needed.

We thank J. B. Oke for information about the AB system. One of us (M. S.) would like to acknowledge the hospitality of the Institute for Advanced Study at Princeton, New Jersey, during the academic year 1980–1981 where part of this work was performed. This research was supported in part by the National Science Foundation under grants AST-7722615 and AST-8111754.

APPENDIX A

ALTERNATIVE MODELS OF EVOLUTION

Since for redshifts z < 1.8 and B > 18 information about surface densities is very scarce, it is of interest to inquire whether the 4 m grating prism survey yields substantive information based on the next strongest emission line, that of C IV at 1549 Å. We will find that the numbers detected are low. Consequently, we have derived some alternative models of evolution based on a

lower number of high-redshift quasars with B < 19.5 than was adopted in the main text.

First, we investigate whether C IV emission is detected on the original transmission grating prism exposures of quasars showing Ly α emission. For the Hoag-Smith (1977) survey, C IV emission falls in the range of sensitivity of the IIIa-F emulsion for 13 of the quasars with

⁶The single-object analysis employed is costly in computing time since the V_a' computation of the 114 BQS objects in survey areas with 74 different $B_{\rm lim}$ values requires 8436 numerical integrations (see eqs. [17] and [18]).

z>1.8, B<19.5 listed in Table 3. The original grating prism plates showed C IV emission in 10 cases. Similarly, we find that of the three quasars with z>1.8, B<19.5 of the KPNO 4 m survey (Vaucher and Weedman 1980) for which C IV falls in the range of sensitivity of the IIIa-J emulsion, two showed C IV on the original grating prism exposures. We conclude that, for B<19.5, C IV emission has a detection probability on the 4 m grating prism surveys of 0.75.

Since this is a fairly high detection probability, we proceed to search for quasars in the 4 m survey with redshifts in the range 1.3-1.8. The lower redshift limit corresponds to observed wavelength 3560 Å for C IV. We find only four such quasars with B < 19.5 in the two 4 m surveys, where the models presented in the main text predict around 14.

The discrepancy may be due to our overestimating the probability of C IV detection, which may be enhanced by the presence of (stronger) Ly α emission. Whatever the cause of the discrepancy, we did derive some alternative models in which we fitted to the 4 m grating prism detections based on Ly α and/or C IV, over the redshift range 1.3–3.1.

TABLE 13
SURFACE DENSITIES FOR TWO ALTERNATIVE MODELS

				σ (deg^{-2}	
					Mo	dels
Survey	Z	$B_{\rm lim}$	n	Observed	LL1	LHI
Braccesi	0-2.15	18.0	15	0.42	0.28	0.31
Curtis-Schmidt	1.8 - 3.1	18.0	17	0.035	0.12	0.075
4 m grating prism.	1.3 - 3.1	19.5	22	2.9	2.9	2.9
Kron, Chiu	0-3.1	21.0	4	57	30	60

We present in Tables 13, 14, and 15 data for two of these models: LL1 with $M_0 = -22.62$, k = 3.38; and LH1 with $M_0 = -19.76$, k = 1.98. These models predict a surface density for z = 1.8-3.1 and B < 19.5 of 1.6, and $1.2 \, \text{deg}^{-2}$, respectively, much below the value 2.3 $\, \text{deg}^{-2}$ used for the models in the main text. A detailed comparison of Tables 14 and 15 with Tables 8 and 9, respectively, is useful in showing the effect of different adopted surface densities for B < 19.5.

APPENDIX B

LOW-LUMINOSITY QUASARS AND SEYFERT I NUCLEI

The BQS contains 22 objects with $M_B > -23$, of which 12 show some nebulosity on Sky Atlas prints. As mentioned in § III, these objects are low-luminosity quasars and Seyfert nuclei. As the absolute luminosity of these objects decreases, the nebulosity will become relatively stronger, the integrated colors redder, and therefore their probability of inclusion in the BQS (which is made up of dominantly stellar objects) diminishes.

Low-luminosity quasars and Seyfert nuclei (with $M_B > -23$) make up a sizable fraction (19%) of the BQS. Since these low-luminosity objects have a rather shallow evolution in our models, their numbers do not increase as rapidly with magnitude as those of the quasars ($M_B < -23$). As a consequence, e.g., in model HH1 they would contribute only 1-2% of the number of quasars in the range B=18-22.

We mention the above numbers with qualification, since they refer to those objects which at small redshifts appear to be dominantly stellar on Sky Atlas prints (a requirement for inclusion in the BQS). Seyfert galaxies of somewhat lower luminosity may at larger redshifts become stellar in appearance (see Hawkins and Stewart 1981). Hence, the numbers given above are likely to be underestimates.

A comparison of our luminosity function for (stellar) objects with $M_B > -23$ with the luminosity function of Seyfert I galaxy nuclei derived from data given by Véron (1979) shows approximate agreement at $M_B = -21.5$. Since the luminosity function of Seyfert I nuclei is still poorly established, we expect that the BQS may contribute useful statistical information in the range $-23 < M_B < -21$.

APPENDIX C

PURE LUMINOSITY EVOLUTION

Pure luminosity evolution is based on the assumption that the luminosity function is constant at all times, except for a time-dependent shift L(t) in the luminosity coordinate (see eq. [15]). Mathez (1978), Braccesi et al. (1980), and Cheney and Rowan-Robinson (1981) have explored the interpretation of quasar counts on the basis of pure luminosity evolution.

Inspection of model luminosity functions derived in \S VII shows that the parts covered by existing surveys can be brought into approximate coincidence by shifting the luminosity coordinate M_B by around 6τ magnitudes. This is practically identical to the luminosity evolution considered by Mathez (1978) and Cheney and Rowan-Robinson (1981). With such a pure luminosity evolu-

 ${\bf TABLE\ 14}$ Redshift-Magnitude Table $^{\rm a}$ for Model LL1 (see Table 13)

AB(6500) 13.55		14.55		15.55	16.55	17.55	5	18.55	19.55	20.55		21.55	22.55	23.55	24.55
B14		15		16	17	18		16	20	21		_,	73	24	25
$z = 5.0 \dots$					9	2100	, ,			-	, <u>S</u>	;	*		
7 = 4 5	0.000		0.0000	0.0000	2	0.016	0.10		0.1	7:1	2	37		17	71
	0.0000		0.0000	0.0000	00	0.014	0.15	0.0	7 J	3.5	91	21		81	∞
1.0	0.0000		0.0000	0.0010	01	0.020	0.18	9.0	9	4.3	50	15	_	2	4
2	0.0000		0.0000	0.0034	4	0.028	0.29	9.0	9	4.6	16	13		6	_
2 – 3.0	0.0000		0.0000	0.0029	67	0.036	0.19	1.4	4	7.7	6	6		4	0
	0.0000		0.0004	0.0044	4	0.053	0.17	1.5	2.5	6.3	9	9		_	0
z – z.o	0.0000		0.0003	0.0054	4	0.028	0.32	2.4	4	3.1	4	2		0	0
7 - 1.5	0.0000		0.0005	0.0046	93	0.051	0.52	1.1	_	2.0	2	0	,	0	0
	0.0000		0.0005	0.0102		0.090	0.28	9.0	, ,	0.5	0	0	*	0	0
$z = 0.0 \dots$	0.0008		0.0038	0.0159	69	0.046	0.08	0.0	0	0.0	0	0	•	0	0
N(z < 3.5)	0.0008		0.0056	0.0468		0.332	1.85	9.7		24.3	37	30		14	-
											-	-			

^a Entries are n(B, z) per sq. deg.

TABLE 15 REDSHIFT-MAGNITUDE TABLE^a FOR MODEL LH1 (see Table 13)

AB(6500) 13.55 B 14	2	14.55		15.55 16		16.55 17	17.55 18	-	18.55	19.55 20		20.55 21	21.55 22	22.55 23		23.55 24	44	24.55 25
z = 5.0	0.0000		0.0000	, o	·0.0000.	900:0		0.04		0.4	7.0	10		63	135	-	248	
$z = 4.5 \dots$	0.0000		0.0000	0	0.0000	0.006		0.07	-	0.4	2.5	22	· ·	26	- 153		213	
$z = 4.0 \dots$	0.0000		0.0000	0	0.0005	0.010		0.08		0.3	3.5	32		62	149		130	
$z = 5.5 \dots$	0.0000		0.0000	0	0.0018	0.015		0.15	-	0.4	4.6	30	,	73	147		42	
$z = 3.0 \dots$	0.0000		0.0000	0	0.0019	0.021		0.11		1.1	11.2	27		77	100		0	
z = 2.5	0.0000		0.0003	0	0.0032	0.033		0.12		1.5	11.0	30		02	27		0	
$z = 2.0 \dots$	0.0000		0.0003	0	0.0042	0.019		0.28		3.5	9.4	30	-	33	0		0	
$Z = I.S \dots \dots$	0.0000		0.0005	0	0.0038	0.045		0.67		2.5	8.6	16	, ,	-,	0		0	
$z = 1.0 \dots$	0.0000		9000.0	0	0.0105	0.113		0.56		2.3	3.4	0		0	0		0	
$z = 0.0 \dots z$	0.0007		0.0038	0	0.0194	0.079		0.20		0.1	0.0	0			0		0	
N(z<3.5)	0.0008		0.0056	0	0.0449	0.326		2.09	1	11.3	49.5	133		254	273		43	
										÷								

^aEntries are n(B, z) per sq. deg.

tion, BQS objects in the observed range $-30 < M_B < -21$ yield a local luminosity function $\Phi(M_B(0),0)$ in the range $-25 < M_B < -20$.

For $q_0 = 0.1$ we can fit both the Braccesi and 4 m grating prism samples by adopting $\Delta L = 6.3\tau$ mag. We obtain a surface density N(B < 21) = 29 deg⁻², identical to the low alternative value considered in the main text. However, objects that in the BQS have $-23 < M_B < -21$ contribute 22 deg⁻² of this surface density. Our qualifications about the use of these objects from the BQS, discussed in Appendix B, apply here, too.

For $q_0 = 0.5$ we find that for $\Delta L = 5.8\tau$ mag we can fit the low (L) surface density of the 4 m surveys (see Appendix A), but then predict for the Braccesi survey

0.67 deg⁻² or 40% more than observed. At B=21 the surface density is 14 deg⁻², far less than observed. Extrapolating the luminosity function $\Phi(M_B(0),0)$ beyond the range covered by the BQS, to $M_B(0)=-19$ or -18 should suffice to boost N(B<21) to the observed range of 30-60 deg⁻².

In the case of pure luminosity evolution, the statistics of faint quasars with observed luminosity $M_B < -23$ are dominated by objects that evolve into or correspond to nuclei of Seyfert galaxies at the present epoch. Further studies will benefit from improved knowledge about the luminosity function of Seyfert galaxy nuclei (see Véron 1979), especially at lower luminosities.

REFERENCES

```
Avni, Y. 1981, Ap. J. (Letters), 248, L95.
Avni, Y., and Bahcall, J. N. 1980, Ap. J., 235, 694.
Berger, J., and Fringant, A.-M. 1977, Astr. Ap. Suppl., 28, 123.
Blake, G. M. 1978, M.N. R.A.S., 183, 21P.
Boroson, T. A., Oke, J. B., and Green, R. F. 1982, Ap. J., 263, 32.
Braccesi, A., Formiggini, L., and Gandolfi, E. 1970, Astr. Ap., 5, 264.
Braccesi, A., Lynds, R., and Sandage, A. 1968, Ap. J. (Letters), 152, L105.
Braccesi, A., Zitelli, V., Bonoli, F., and Formiggini, L. 1980, Astr. Ap., 85, 80.
Carswell, R. F., and Smith, M. G. 1978, M.N. R.A.S., 185, 381.
Cheney, J. E., and Rowan-Robinson, M. 1981a, M.N. R.A.S., 195, 497.

——. 1981b, M.N.R.A.S., 195, 831.
Chiu, L.-T. G. 1980, Ap. J. Suppl., 44, 31.
Downes, R. A., and Margon, B. 1981, A.J., 86, 19.
Eddington, A. S. 1940, M.N. R.A.S., 100, 354.
Green, R. F., and Morrill, M. E. 1978, Pub. A.S.P., 90, 601.
Green, R. F., and Schmidt, M. 1978, Ap. J. (Letters), 220, L1.
Green, R. F., and Schmidt, M. 1978, Ap. J. (Letters), 220, L1.
Green, R. F., Schmidt, M., and Liebert, J. L. 1983, in preparation.
Hawkins, M. R. S., and Stewart, N. J. 1981, Ap. J., 251, 1.
Hayes, D. S., and Latham, D. W. 1975, Ap. J., 197, 593.
Hewitt, A., and Burbidge, G. 1980, Ap. J. Suppl., 43, 57.
Hoag, A. A., and Smith, M. G. 1977, Ap. J., 217, 362.
Koo, D. C., and Kron, R. G. 1982, Astr. Ap., 105, 107.
Kron, R. G., and Chiu, L.-T. G. 1981, Pub. A.S.P., 93, 397.
Lewis, D. W., MacAlpine, G. M., and Weedman, D. W. 1979, Ap. J., 233, 787.
Lynds, R., and Wills, D. 1972, Ap. J., 172, 531.
Masson, C. R., and Wall, J. V. 1977, M.N.R.A.S., 180, 193.
Mathez, G. 1978, Astr. Ap., 68, 17.
Mattig, W. 1958, Astr. Nach., 284, 109.
Morgan, W. W. 1972, in IAU Symposium 44, External Galaxies and Quasi-stellar Objects, ed. D. S. Evans (Dordrecht: Reidel), p. 97.
Noguchi, T., Maehara, H., and Kondo, M. 1980, Ann. Tokyo Astr. Obs., Vol. 18, No. 1.
Oke, J. B. 1974, Ap. J. Suppl., 27, 21.
```

RICHARD F. GREEN: Steward Observatory, University of Arizona, Tucson, AZ 85721

MAARTEN SCHMIDT: Department of Astronomy 105-24, California Institute of Technology, Pasadena, CA 91125

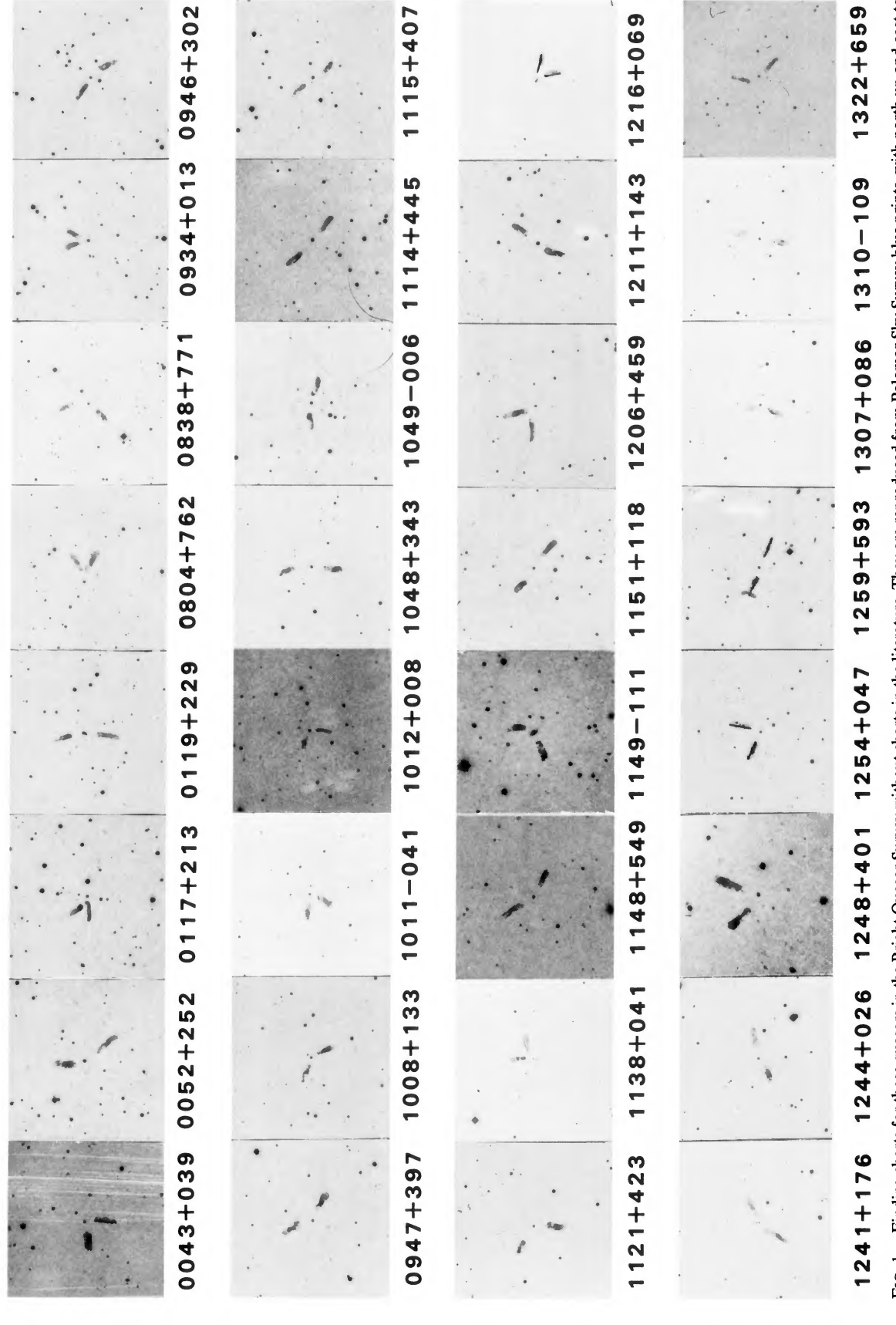


Fig. 1.—Finding charts for those quasars in the Bright Quasar Survey without charts in the literature. They are reproduced from Palomar Sky Survey blue prints, with north up and east to the left, and are approximately 11.4 on a side.

SCHMIDT AND GREEN (see page 354)

